MCP Papers in Press. Published on April 11, 2005 as Manuscript M400182-MCP200

Proteome Dynamics during C2C12 Myoblast Differentiation

Thomas Kislinger[1]*, Anthony O. Gramolini[2]*, Yan Pan[2]*[@], Khaled Rahman[1$],

David H. MacLennan[2], and Andrew Emili[1,2#]

[1]Program in Proteomics and Bioinformatics, University of Toronto, Toronto, ON, Canada;

[2]Banting and Best Department of Medical Research, University of Toronto, Toronto, ON, Canada

[@]Present address: Protana Inc., 251 Attwell Drive, Toronto, ON, Canada

[$]Present address: Department of Biochemistry and Molecular Biology, University of Calgary, 3330 Hospital Drive, Calgary, AB, Canada

*contributed equally to this work

[#]Corresponding author: CH Best Institute
112 College Street, Room 402
Toronto, Ontario Canada M5G 1L6
Tel: 416-946-7281 / Fax: 416-978-8528
e-mail: andrew.emili@utoronto.ca

Running Title: Proteome Dynamics during C2C12 Myoblast Differentiation

Keywords: muscle, myoblast, proliferation, differentiation, myocyte, protein expression, profiling, shotgun sequencing, tandem mass spectrometry, proteome, dynamics.

SUMMARY

Mouse-derived C2C12 myoblasts serve as an experimentally tractable model system for investigating the molecular basis of skeletal muscle cell specification and development. To examine the biochemical adaptations associated with myocyte formation comprehensively, we have used large-scale gel-free tandem mass spectrometry to monitor global proteome alterations throughout a time-course analysis of the myogenic C2C12 differentiation program. The relative abundance of ~1,800 high confidence proteins was tracked across multiple time-points using capillary-scale multi-dimensional liquid chromatography coupled to high-throughput shotgun sequencing. Hierarchical clustering of the resulting profiles revealed differential waves of expression of proteins linked to intracellular signaling, transcription, cytoarchitecture, adhesion, metabolism and muscle contraction across the early, mid and late stages of differentiation. Several hundred previously uncharacterized proteins were likewise detected in a stage-specific manner, suggesting novel roles in myogenesis and/or muscle function. These proteomic data are complementary to recent microarray-based studies of gene expression patterns in developing myotubes, and provide a holistic framework for understanding how diverse biochemical processes are coordinated at the cellular level during skeletal muscle development.

INTRODUCTION

Skeletal muscle consists of tightly bundled cylindrical multinucleated myocytes, each packed with ordered tandem arrays of actin-myosin contractile filaments, which together account for nearly 40% of the total mass of the human body. These highly differentiated cells originate late in embryogenesis from somite-derived mesenchymal myoblast precursor cells in a multi-step pathway initiated in response to inductive physiological cues (1). Activation of the myogenic program is normally tightly coupled to a network of signal transduction pathways that act to repress or stimulate cell proliferation and differentiation during embryonic development (1). These pathways function, at least in part, by altering the levels of critical target regulatory proteins through both transcriptional and post-transcriptional mechanisms (1). However, the developmental transitions responsible for myoblast commitment, myocyte specification and possible developmental plasticity are not fully understood and are just now beginning to be described in integrated molecular terms (2).

Cultured undifferentiated fibroblast-like mouse and human myoblast cell lines serve as excellent model systems for investigating the complex biochemical adaptations that underlie the formation of functional myocytes. In the absence of mitogenic stimuli, proliferating myoblasts synchronously withdraw from the cell cycle, elongate, adhere and finally fuse together to form myotubes exhibiting most, if not all, of the principle mechano-biochemical adaptations associated with contractility (1). Molecular genetic studies of this myogenic program have provided fundamental insight into key regulatory events associated with this profound resetting of cell physiology (2). These include the discovery of critical intracellular signaling pathways and their target sequence-specific transcriptional factors which control cascading waves of gene expression in terminally differentiating myoblasts, leading to large-scale biological reorganization and the formation of functional myofibrils (3,4). Nonetheless, knowledge of the full range of biochemical

adaptations associated with myocyte formation remains incomplete, masking the complexity that is likely to exist *in vivo*.

Genome-scale molecular profiling studies offer a unique opportunity to investigate the molecular hierarchy and logic that governs muscle cell development and physiology. To this end, several groups have reported the use of DNA-based microarray technology to examine global patterns of transcription in cultured myoblasts during the transition from mitotic cell proliferation to terminal differentiation (5-7). These studies have provided evidence of significant changes in gene expression patterns during myogenesis. However, since mRNA transcript levels do not always correlate with corresponding cognate protein abundance (8), determination of the full spectrum of biochemical alterations associated with skeletal muscle formation might be best ascertained by monitoring alterations in protein abundance and turnover directly (9,10).

Systematic comparison of changes in the proteome composition of mitotic and differentiating myoblasts should also provide insight into the various mechanisms and pathways that underlie the formation of skeletal muscle. To this end, Raghow and colleagues used two-dimensional gel-electrophoresis (2D-PAGE)-based proteomic methods to compare the levels of soluble proteins in mitotic and fully differentiated C2C12 mouse myoblasts (11). Although several notable alterations in protein abundance were uncovered, overall the proteome adaptations detected were surprisingly slight and less dynamic than widely assumed. Given that gel-based methods have limited sensitivity, modest dynamic range and substantive detection biases (12,13), it is likely that many of the proteome perturbations associated with the muscle differentiation program went undetected, particularly those associated with lower abundance proteins.

Recent advances in alternative gel-free proteome profiling methods, combining liquid chromatography with ultra-sensitive tandem mass-spectrometry-based peptide sequencing (LC-

MS), offer a complementary and likely more effective experimental approach for examining global changes in protein expression as a function of development (14,15). Here, we report the results of an extensive LC-MS-based shotgun profiling analysis of alterations in protein expression in differentiating C2C12 myoblasts as a function of the myogenic program. Striking changes were detected in the abundance of hundreds of proteins linked to cell adhesion, intracellular signaling, gene expression, metabolism and muscle contraction, consistent with a substantive and highly dynamic, biochemical remodeling of cell function. These data were broadly consistent with the predictions reported by a recent microarray-based study of myogenic gene expression by Tomczak *et al.* (7), and provide compelling evidence for the involvement of previously overlooked transcription regulators, signaling factors and adhesion molecules, as well as novel uncharacterized proteins, in skeletal muscle development and contractility.

EXPERIMENTAL PROCEDURES

Materials

Ultrapure-grade urea, ammonium acetate, ammonium bicarbonate, dithiothreitol (DTT), ethylene-diamine-tetracetic acid (EDTA), iodoacetamide, and calcium chloride were obtained from Sigma-Aldrich (St. Louis, MO). Heptafluorobutyric acid (HFBA) was obtained from BioLynx (Brockville, ON, Canada). Poroszyme bead immobilized trypsin was purchased from Applied Biosystems (Streetsville, ON, Canada). Sequencing-grade Endoproteinase Lys-C was obtained from Roche Diagnostics. High performance liquid chromatography (HPLC)-grade acetonitrile, methanol and distilled water were obtained from Fisher Scientific. SPEC Plus PT C18 solid phase extraction pipette tips were purchased from Ansys Diagnostics (Lake Forest, CA). Tissue culture media, serum, media supplements and plasticware were obtained from GIBCO-BRL/Life Technologies (Burlington, ON).

Cell Culture and protein preparation

Mitotic C2C12 mouse myoblasts (American Type Culture Collection (ATCC), Manassas, VA) were passaged as subconfluent monolayers in Dulbeco modified Eagle medium (DMEM; GIBCO-BRL; Burlington, Ontario, Canada) supplemented with 20% fetal bovine serum, 200 mM L-glutamine, 10 U/ml penicillin, and 10 μg/ml streptomycin. Confluent (90%) myoblasts were differentiated into myotubes by culturing the cells in DMEM supplemented with 2% horse serum. Crude nuclear extracts of harvested cells were prepared using a commercial kit (Nu-CLEAR™ Extraction kit; Sigma-Aldrich). Briefly, cell pellets were resuspended in five volumes of hypotonic lysis buffer (10 mM HEPES, pH 7.9, 1.5mM $MgCl_2$, 10 mM KCl) and incubated on ice for 15 minutes. The suspension was centrifuged for 5 minutes at 420 g and the resulting pellet was

resuspended in 400 µl of lysis buffer. The cells were disrupted using a glass tissue homogenizer with a type B pestle and centrifuged for 20 minutes at 1,000 g. The crude nuclear pellet was resuspended in extraction buffer (20 mM HEPES, pH 7.9, 1.5 mM MgCl2, 0.42 M NaCl, 0.2 mM EDTA, 25% glycerol) and incubated for 30 minutes with gently shaking followed by several strokes with a glass pestle. The suspension was centrifuged for 5 minutes at 21,000 g, with the crude nuclear extract supernatant used for further analysis.

Protein digestion

Aliquots of extract (150 µg total protein) were precipitated with 5 volumes of ice-cold acetone overnight at -20°C. The precipitate was centrifuged for 20 minutes at 21,000 g and the pellet dissolved in solubilization buffer (8M urea, 50 mM Tris-HCl, pH 8.5, 2 mM DTT) for 1 hour at 37°C. The soluble proteins were alkylated with 5 mM iodoacetamide, diluted to 4 M urea with 50 mM ammonium bicarbonate, pH 8.5, and then digested overnight with endoproteinase Lys-C at 37°C. The following day, the samples were further diluted to 2 M urea with 50 mM ammonium bicarbonate, pH 8.5, supplemented with $CaCl_2$ to a final concentration of 1 mM, and digested overnight with Poroszyme immobilized trypsin beads at 30°C with rotation. The resulting peptide mixtures were desalted using solid phase extraction with SPEC-Plus PT C18 cartridges according to the manufacturer's instructions, and stored at -80°C until further use. Sample pH was made < 3 by adding formic acid prior to LC-MS analysis.

Multidimensional Protein Identification Analysis

The MudPIT shotgun profiling methodology reported by Washburn *et al.* (16) was used essentially as described in Kislinger *et al.* (17). Briefly, a Surveyor quaternary HPLC-pump (Thermo Finnigan, San Jose, CA) was interfaced with a Finnigan LCQ DECA XP ion trap tandem

mass spectrometer. A 150 μm i.d. fused silica microcapillary column (Polymicro Technologies; Phoenix, AZ) was pulled using a P-2000 laser puller (Sutter Instruments; Novato, CA) and packed with ~10 cm of 5 μm Zorbax Eclipse XDB-C_{18} (Agilent Technologies, Inc.; Mississauga, ON, Canada) followed by ~6 cm of 5 μm Partisphere strong cation exchange (SCX; Whatman, Clifton, NJ). Samples were loaded manually onto a separate column using a pressure vessel, with the loaded column then connected to the HPLC pump using a PEEK microcross. Each sample was analyzed via a fully automated 15-cycle data-dependent chromatographic analytical method using a low flow (<300 nl/min) set-up essentially as described (17).

Informatics

Over 250,000 uninterpreted product ion mass spectra were sequence mapped against a locally maintained, minimally redundant database of human and mouse protein sequences (Swiss-Prot and TrEMBL; downloaded from the European Bioinformatics Institute) using the SEQUEST database search algorithm (18) running on a multi-processor computer cluster;a static modification mass of +57 amu was added to all cysteine residues. The false-discovery rate was estimated by also searching against an equivalent number of reversed non-sense protein sequences (17). Putative protein sequence matches were evaluated statistically using STATQUEST, a Perl-base computer algorithm that employs an error-estimation model to compute the accuracy of individual predictions so as to minimize the false discovery rate (17). A stringent threshold cut-off (*P*-value <0.05), corresponding to a 95% or greater likelihood that a given protein was correctly identified, was used to filter the datasets. The 1,865 high confidence proteins were then sub-grouped into specific functional categories based on the Gene Ontology (GO) annotation schema (19) using the Perl-based computer program GOClust (17). 1,487 proteins (80%) were linked to one or more GO terms: 1,138 proteins (61%) mapped to the principle GO category *biological process*, 1,316

proteins (71%) mapped to the GO category *molecular function*, while 1,184 proteins (64%) mapped to the GO category *cellular component* (**Supplementary Table S1)**

Hierarchical Clustering, Data Visualization and Cluster Evaluation

The total cumulative spectral count recorded from each protein was interpreted as a semi-quantitative measure of relative abundance (20). For the time-course analysis, relative protein abundance was estimated by calculating the ratio of the natural logarithm of total spectra detected for each protein relative to that detected in the undifferentiated, asynchronously proliferating (day 0) myoblast cell population. Use of the log-scale allows negative expression ratios to be more readily visualized as a fold-change rather than fractional (simple ratio) data. It also tightens the spread of the data points, allowing for more subtle local differences to be detected across a broader dynamic range. Hierarchical clustering was carried out using the Cluster 3.0 freeware software package using the Correlation distance metric with average linkage selected. To improve data grouping, a nominal low, non-zero cut-off value (0.01) was substituted for blank values in cases where a protein was not detected in a particular sample. The clustered data profiles were visualized in heat map format using the TreeView software package (21).

Statistical enrichment of proteins matching to select functional categories (GO terms) within each of the clusters was assessed using the hypergeometric distribution (22), which reflects the probability (*P*-value) that the intersection of a given protein list with any given annotation term occurs by chance. A Bonferroni amendment factor was used to correct for multi-hypothesis testing; the *P*-value deemed significant for an individual test was determined by dividing the preliminary value by the number of tests conducted, thereby accounting for spurious significance due to repeat testing over all the categories in the GO database. A threshold cutoff value of 10^{-3} was used as a final selection criterion to highlight promising, biologically interesting clusters.

Proteomic and microarray dataset comparisons

The complete supplementary gene expression datasets from the microarray study of Tomczak *et al.* (7), which was based on the mouse MG_U74Av2 and MG_U74Cv2 Affymetrix GeneChip platforms (Santa Clara, CA), were parsed into a relational database. Cross-comparison of the respective genomic and proteomic profiles was carried out by first cross-referencing the respective cognate gene products by mapping SwissProt/TrEMBL accessions using annotation tables downloaded from the Affymetrix website. The scaled microarray data was then aligned and co-clustered with the proteomic patterns using the Spearman distance metric. To correct for differences in experimental design and slight temporal shifts, the entire microarray dataset was normalized by dividing each data point by the value recorded for either day –2 or day 0 according to the nomenclature of Tomczak *et al.* (7), while the day 0 proteomic time-point was used as the reference for calculating the ratio of protein expression. The entire set of mapped gene protein pairs with their corresponding data values is presented in **Supplement Table S2**.

Reverse-transcription polymerase chain reactions (RT-PCR)

Total RNA was extracted from cells using Tripure (Boehringer, Indianapolis, IN). Total RNA (100 ng) was used for RT-PCR, essentially as described (23). cDNAs were amplified using specific primer pairs based on available NCBI sequence data (**Supplemental Table S3**) and visualized on 1% agarose gels. Between 22 and 32 amplification cycle numbers were used per reaction to ensure linearity of response.

RESULTS

Proteomic investigation of an *in vitro* model of myogenesis

A temporally well-defined myogenic differentiation program can be triggered selectively in cultured C2C12 myoblasts upon withdrawal of media-derived growth factors and mitogens (23). When switched to differentiation medium (see *EXPERIMENTAL PROCEDURES*), mitotic C2C12 myoblasts rapidly cease proliferating and initiate a synchronously terminal differentiation program (**Figure 1**). The cells also exhibit striking morphological changes over the course of 2-6 days, eventually fusing into mature multinucleated myotubes (i.e. by day 6).

To investigate the global dynamics of protein expression occurring during myogenesis, we used a variant of the gel-free multidimensional protein identification technology (a.k.a. MudPIT), first pioneered by Yates and colleagues (16) and adapted and optimized for large-scale profiling of mammalian cells and tissue by our group (17). Nuclear-enriched protein fractions were isolated from both proliferating C2C12 myoblasts (MB) and from differentiating myotubes (MT) harvested at four different time points (2, 4, 6 and 10 days post serum withdrawal) following induction of the differentiation program. The samples were digested with endoproteinase LysC and trypsin extensively, and the peptide mixtures analyzed by multiple rounds of capillary-scale multidimensional liquid chromatography coupled online to data-dependent fragmentation using a fully automated ion trap instrument (16). This efficient and highly sensitive method of proteome mapping circumvented many of the limitations associated with more traditional 2D gel-based proteomic technology (24), enabling a far more comprehensive characterization of lower abundance proteins in particular (16,17).

Approximately 50,000 fragmentation spectra, encompassing >5,000 peptides selected for collision-induced dissociation, were acquired for each protein fraction. The database search algorithm SEQUEST (18) was used to match these spectra to peptide sequences present in a

minimally redundant database of mouse and human proteins obtained from Swiss-Prot/TrEMBL (25). The probability assessment algorithm STAQUEST (17) was then used to assign a statistical confidence score to each putative candidate identification. In practice, due to the non-linear distribution of database confidence scores, the majority of the predictions had extremely high likelihoods of being correct. As seen in **Supplementary Figure S1**, the majority of database matches had predicted likelihood scores of greater than 99%. As an independent quality measure, the preponderance of incorrect (false positive) matches was empirically calculated by populating the reference database with an equal number of mock decoy proteins, created by inverting the amino acid orientations of the normal Swiss-Prot/TrEMBL protein sequences. Matches to these "reverse" sequences represent spurious false positives since these they are not expected to occur naturally. The final proportion of matches mapping to reverse proteins relative to normal (or "forward") proteins provided an objective criterion for estimating the false-discovery rate.

Quality filtering of large-scale expression datasets represents a trade-off between specificity (precision), which reflects the proportion of correct identifications, and sensitivity (recall), which indicates the bone fide proteomic coverage attained. Receiver-Operator-Characteristic (ROC) plots are often used to assess the effects of varying classification criteria on classification precision and recall. Although prior knowledge of the correct class labels is not available (since we do not know a priori which proteins are in fact present in the samples), in practice, one can estimate this trade-off empirically based on the fraction of database matches to the "forward" and "reverse" sequences after applying various quality filters. The ROC-like plot shown in **Supplementary Figure S2** shows the effects of applying confidence filters of different stringency to the time-course datasets.

To ensure dependable accuracy, we opted to apply a stringent first-pass probability filter (albeit at the expense of reduced detection coverage) corresponding to a minimum of ≥95% confidence to each candidate peptide match. This stringent filtering resulted in the detection of

1,865 high confidence (*P*-value <0.05) proteins throughout the myogenic differentiation program. Importantly, only ~2.5% 'reverse' decoy proteins passed this criteria (data not shown), confirming its reliability. A summary of the final dataset is shown in **Table 1**, while a breakdown of the spectral counts detected per protein per time point is provided in **Supplementary Table S4;** a complete description of the search results (including peptide sequence, precursor ion mass and charge, and the search algorithm and actual confidence scores) is provided in **Supplementary Table S5**. Several hundred of these high confidence proteins appear to be muscle lineage-specific as they were not detected in previously reported extensive proteomic analyses of unrelated mouse tissues, such as lung and liver [(17); data not shown]. These included a surprisingly large fraction (~250) of uncharacterized proteins (i.e. "hypothetical", "unknown", or simply labeled as "Riken" cDNA products). Since spurious database matches often have limited supporting evidence, usually corresponding to only a single spectral match, appropriately labeled MS/MS spectra corresponding to all high confidence protein identifications based on single-peptide assignments highlighted in this study are provided in **Supplementary Figure S3** to support the biological conclusions drawn.

Data clustering and visualization

To better monitor changes in the global pattern of protein expression throughout the differentiation program, we next applied large-scale data clustering and visualization algorithms, used widely to monitor genome-wide differences in gene expression (21,26), across the entire set of proteomic profiles. Changes in relative protein abundance were estimated based on the observed ratio of total spectra matching each protein detected in the four differentiation time-points, relative to the starting undifferentiated cell population (see *EXPERIMENTAL PROCEDURES*). Hierarchical clustering of the resulting expression profiles (**Figure 2**) revealed successive, overlapping clusters of proteins that were either induced (up-regulated) as a function of the

differentiation program, or whose relative abundance diminished (down-regulated) concomitant with the cessation of cell division.

Since functionally related proteins are often coordinately expressed (26), clusters can be indicative of a shared biological role. Hence, we examined cluster membership for evidence of similar biological properties based on enrichment for Gene Ontology (GO) annotation terms describing protein molecular function, biological roles and/or molecular environment (19). Statistical enrichment was assessed using a hypergeometric distribution test (22) together with a correction factor for multi-hypothesis testing [see *EXPERIMENTAL PROCEDURES*], to estimate the significance of deviations in protein classification. Low P-values ($<10^{-3}$, or 0.001) indicated a cluster was significantly enriched for a particular GO term as compared to chance alone.

In this manner, striking changes in protein function were detected throughout the time-course (**Figure 2**). A first major phase followed immediately after initial withdrawal of serum (i.e., day 2) and was represented by a sharp but transient increase in levels of intracellular transporters and transcriptional regulatory factors (labeled as **cluster A**; discussed further below). A second phase, consisting of more gradual waves of expression of cell remodeling factors, such as signaling factors and intercellular adhesion molecules, followed next (**cluster B**). By Day 10, a marked alteration in metabolic capacity and cytoskeletal organization was apparent, including dramatically elevated levels of proteins linked to mitochondrial function, fatty acid oxidation and muscle contraction (**cluster C**), consistent with the gross morphological and physiological transitions associated with terminal differentiation and formation of muscle-like myotubes (27-29). This phase was also accompanied by commensurate down-regulation of enzymes linked to cell division, protein synthesis and active DNA metabolism (**cluster D**), coincident with exit from the cell proliferation cycle and cessation of cell growth.

For a closer examination of alterations in these core processes, the proteins were sorted based on membership to discrete functional categories (GO-terms). Since low spectral counts are more likely to be prone to spurious variance (20), more reliable biological inferences can be drawn by looking for trends across the samples (i.e. functional categories showing altered expression across the differentiation time-points). As outlined below, analyses of the resulting sub-groups helped to highlight biologically-interesting patterns of differential protein expression occurring during progression of the myogenic program.

Protein expression patterns in early myogenic development (dividing myoblasts)

Proliferating myoblasts were found to express 257 proteins preferentially linked to a range of functions associated with cell proliferation, chromosomal replication and the mitotic cell cycle, several of which are listed in **Table 2** (see **Supplementary Table S6** for complete details). These included many proteins mapping to the GO-term ***nucleus*** (53 proteins, including CREB-binding protein, DNA polymerase, and the transcription factor Notch 4); ***cell cycle*** (8 proteins, including Cullin-3, and the Cyclin Dependent Kinase 1 (CDK1); ***DNA replication*** (8 proteins, including replication factors MCM4 and DNA primase; and ***chromosome*** (6 proteins, including High Mobility Group protein 4, Telomeric Repeat Binding Factor 2, and the serine/threonine protein kinase splicing factor PRP4).

Additional categories were found to be statistically-enriched in the dividing myoblasts (**Supplementary Table S6**), most notably the GO-term ***DNA binding*** (25 proteins, including the chromosome-associated kinesin KIF4A, nuclear factor Hcc-1 and TATA-binding protein factor 2N); ***protein biosynthesis*** (17 proteins, including subunits of translation initiation factor 3, and multiple 60S ribosomal proteins)*;* ***RNA binding*** (16 proteins, such as fragile X mental retardation protein 1 homolog, ATP-dependent RNA helicase p54, and heterogeneous nuclear

ribonucleoprotein M); and ***cytoskeleton*** (7 proteins, including α-centractin, dynactin complex 50 kDa subunit, radixin and profilin I).

Expression patterns during early-stage induction of the differentiation program

Substantive changes in protein levels were detected immediately following induction of the myogenic program (day 2) by withdrawal of serum-derived mitogens, consistent with a major shift from cell division to terminal differentiation. Many of these proteins were detected exclusively at this stage, several of which are listed in **Table 3**. These included marked up-regulation of proteins mapping to select functional categories (see **Supplementary Table S7** for complete details), including the GO terms ***nucleus*** (55 proteins, such as vitamin D3 receptor, CpG binding protein, mRNA capping enzyme (HCE), and ATP-dependent chromatin remodeling protein); ***DNA dependent regulation of transcription*** (20 proteins, including the Kruppel-like factor 4, homeobox protein Meis1, nuclear receptor corepressor 1, mothers against decapentaplegic (SMAD) 4, lamin B receptor); and ***protein binding*** (35 proteins, such as neurogenic locus notch homolog protein 3, syntaxin4, Rab6-interacting protein 2 isoform, myosin 5 and thyroid receptor interacting protein).

Changes in expression associated with myotube formation

Viewed collectively, proteins up-regulated during the differentiation response (days 2-10) were enriched for a number of functional categories (see **Supplementary Table S8** for complete details), including the GO terms ***nuclear*** (159 proteins; such as homeobox proteins SIX1 and 4, E-box binding transcription factors 4 and 12, ATP-dependent RNA helicase, emerin, GA binding protein, and lamin B1); ***mitochondrion*** (78 proteins, including acyl-CoA dehydrogenases, ATP synthases, cytochrome c oxidase, NAD(P) transhydrogenase, fumarate hydratase, isocitrate dehydrogenase, malate dehydrogenase, superoxide dismutase and ubiquinol-cytochrome-c

reductase complex); ***calcium ion binding*** (43 proteins, such as calnexin, calsequestrin 1, fibulin-1 and -2, protein kinase C, and nidogen 1 and 2); ***cell adhesion*** (29 proteins, including cadherin-13 precursor, fibronectin, and integrins; ***cytoskeleton*** (23 proteins), such as vimentin, dystroglycan, focal adhesion kinase 1, and plakoglobin, α- and β-sarcoglycan, and α-syntrophin); and ***muscle development*** (19 proteins, including skeletal muscle actin, desmin, myosin light chain 1, myosin heavy chain, myosin-binding protein H, troponin C, troponin T, and creatine kinase).

Down-regulated cellular functions

Table 5 highlights notable proteins belonging to several major functional categories significantly down-regulated as a function of cessation of cell division and the process of cell differentiation. These categories included ***cell cycle*** (22 proteins, such as cyclin T, cyclin-dependent kinase 1, cullin-3, and septins 2, 5-7 and septin-like protein Sint1); ***DNA replication*** (16 proteins, including DNA replication licensing factors MCM 2-4, 6 and 7, and various chromatin assembly factors); and ***DNA topoisomerase activity*** (2 proteins, including DNA topoisomerases II alpha and beta isozyme); and ***chromatin*** (9 proteins, such as high mobility group 1 and 2 proteins, SWI/SNF related matrix-associated actin-dependent regulator of chromatin subfamily C member 1, histone deacetylase 1, and Tousled-like kinase). The largest decreases occurred for proteins involved in protein synthesis and mRNA processing during later stages of myotube formation, consistent with the reduced growth rate of the post-mitotic cells (see **Supplementary Table S9** for complete details).

Protein expression patterns in fully differentiated myotubes

As outlined in **Table 6**, a number of proteins were detected exclusively in the fully terminally differentiated (day 10) myotubes (see **Supplementary Table S10** for details). This set

showed significant enrichment for the GO-terms ***mitochondrion*** (41 proteins, such as electron transfer flavoprotein subunits, short chain 3-hydroxyacyl-CoA dehydrogenase, peroxiredoxin 5, and ubiquinol-cytochrome-c reductase complex 11 kDa protein); ***oxidoreductase activity*** (23 proteins, including fatty aldehyde dehydrogenase, heme oxygenase 1, thioredoxin-dependent peroxide reductase, and prostaglandin G/H synthase 1); ***electron transport*** (12 proteins, including Acyl-CoA dehydrogenase, long- and short-chains, cytochrome c oxidase, NAD(P) transhydrogenase, and inducible nitric oxide synthase); ***fatty acid metabolism*** (9 proteins, including Acyl-coenzyme A oxidase 1, short chain 3-hydroxyacyl-CoA dehydrogenase, long-chain-fatty-acid-CoA ligase 3, and hydroxyacyl-coenzyme A dehydrogenase); and ***cell adhesion molecules*** (10 proteins, including cadherin-13, integrin alpha-V, laminin alpha-2, laminin beta-1, CD9 antigen, and vitronectin). These patterns are consistent with the cellular requirements of contractile tissue.

Independent evaluation of gene expression profiles using RT-PCR

In a final set of confirmation experiments, we assessed the mRNA expression patterns of gene products predicted to be differentially expressed by our proteomic screening during the transition from myoblast to early stage myotubes. For these studies, we performed reverse-transcription polymerase chain reactions (RT-PCR) using total RNA isolated from the cell cultures for specific amplification of gene transcripts corresponding to 5 select transcription factors identified as differentially regulated. One of these transcription factors appeared to be either down-regulated at the protein level during myogenesis (SMAD3), while 3 were apparently up-regulated in the myotube stage (Notch-3, homeobox proteins SIX1 and SIX4).

As seen in **Figure 3**, the RT-PCR data correlated well with the proteomics results, since in most instances the time-points producing the most intense RT-PCR products were largely the same as those for which the most elevated proteomic count was recorded. Consistent findings were

observed for SIX1, SIX4, SMAD3, and Notch3. Nevertheless, some lag was observed between the relative gene product abundance as predicted by LC-MS and RT-PCR (e.g. protein and mRNA species). While we cannot exclude sampling error, these temporal shifts most likely reflect differences between mRNA and protein accumulation as well as post-translational control mechanisms (8,30).

Comparison to DNA microarray analyses of global patterns of gene expression

Several microarray studies investigating the global pattern of gene expression in cultured C2C12 myoblasts during virtually identical myogenic differentiation programs have been published (5-7). We compared our proteomic profiles to the results of the most recent and comprehensive study reported by Tomczak *et al.* (7), who used the popular Affymetrix GeneChip platform to investigate changes in mRNA levels using a virtually identical differentiation time course analysis. Using database accession (SwissProt/TrEMBL) cross-references, we were able to map and directly compare the proteomic and genomic expression patterns of 547 pairs of cognate protein-mRNA gene products detected in both studies. In cases where corroborating microarray data confirmed gene product expression (see below), we opted to use a slightly lower preliminary confidence threshold cut-off (i.e. 85%+ confidence, with positive mRNA transcript detected in a published companion microarray study), with the logical expectation that the number of false positives is greatly reduced in this overlapping set.

Co-clustering of the respective time-course profiles revealed good overall concordance in the respective time course patterns (**Figure 4A**). 497 (91%) of the gene products showed similar temporal trends in expression (i.e. elevated or depressed levels as a function of terminal differentiation) in response to myogenesis, after normalizing the microarray data using either the day -2 (**Figure 4A**) or day 0 (**Figure 4B**) time-points as reference to correct for minor differences

in translation lag. The coordinately up-regulated gene products were found to be significantly enriched in GO-terms related to muscle function, such as ***muscle development, calcium ion binding*** and ***muscle contraction***. In contrast, a large co-cluster of down-regulated gene products was found to be enriched for GO-terms related to cell division, such as ***cell cycle, DNA replication*** and ***chromosome***. Although this comparison largely corroborates the microarray and proteomic findings, a closer examination reveals differences in the exact timing of peak abundance in the two datasets, providing evidence of possible post-translational control.

Of the remaining 50 largely discordant gene products (~9% of total mapped), 32 showed reduced protein abundance in the developing myotubes despite evidence for elevated gene expression, whereas 18 showed evidence of protein accumulation despite an apparent reduction in the analogous mRNA transcript level (**Figure 4C**). While experimental noise and artifact could be the basis for these contradictory results, the two clusters were found to be statistically-enriched for several functional categories, including the GO-terms ***cytoskeleton***, ***muscle contraction*** *and* ***actin binding,*** and ***centric heterochromatin***, respectively, suggesting that the differences reflect genuine biological variation in protein accumulation.

DISCUSSION

The development of striated muscle depends on a complex series of integrated mechanisms that ultimately reprogram gene expression and drive cellular reorganization (27-29). This process is initiated through the regulation of a network of intracellular signaling pathways that impinge on select sequence-specific myogenic transcription factors (1,31-34). While traditional reductionist methods have helped researchers to elucidate key mechanistic aspects of the myogenic program, the development of global expression profiling methods now offer the opportunity to investigate this multi-layered process from a holistic, systems-wide perspective.

In this study, we have aimed to provide as complete, and unbiased as possible, a molecular overview of the biochemical adaptations associated with the formation of functional myocytes by examining systematically the temporal dynamics of protein expression in a C2C12 model system using shotgun sequencing. The most striking changes in protein expression detected in response to terminal differentiation occurred during two distinct physiological transitions. The first phase coincided with a rapid withdrawal of the myoblasts from the cell cycle following mitogen deprivation, concomitant with a shift from active proliferation to the initiation of differentiation. This post-mitotic phase was associated with substantive alterations in the levels of a number of critical signaling factors. The second transition consisted of a series of more gradual, but ultimately more profound, perturbations in a broad range of biological systems driving the morphological conversion of single cells into fused, elongated, multinucleated myotubes. This phase included large-scale cytoskeletal rearrangements, enhanced intercellular adhesion, and the maturation of both the contractile apparatus and even entire organelles such as peroxisomes and mitochondria.

Exit from the cell cycle occurs through blockade of the cyclin-dependent kinase (CDK) mitotic engine (35,36), largely through the action of CDK inhibitors (35). Consistent with this expectation, the proliferating myoblast cell population was found to express preferentially high

levels of key activators of mitotic division (**Table 2** and **Supplementary Table S6**), such as CDK1 and Cdc5, without detectable expression of any known CDK inhibitor. On the other hand, the levels of all detectable cell cycle-related proteins decreased markedly following initiation of the differentiation program.

Muscle-specific transcription factors

The major developmental pathways directing skeletal muscle formation are governed by the action of two major classes of transcriptional regulatory factors – namely, the MyoD family of Muscle Regulatory Factors (MRFs) and the Myocyte-specific Enhancer Factor 2 (MEF2) family of MADS-box transcription factors. Each family member encode a basic helix-loop-helix (bHLH) domain that directs binding to specific myogenic DNA regulatory elements, called E-boxes (sequence CANNTG), in response to appropriate physiological signals (37). Three key members of these families were identified in this study (**Supplementary Table S4**), including the myocyte-specific enhancer factor 2D (MEF2D), which was up-regulated significantly in the mid stages of myotube formation (days 2-6), and the MyoD/E-box associated transcriptional co-activators 12 and 4 (Class A bHLH factors ME1 and ME2). MEF2D is known to regulate expression of numerous skeletal-muscle specific genes positively, including creatine kinase and troponin (38,39), which were both detected at elevated levels at later time-points. Nevertheless, we were unable to detect most of the other major myogenic transcription factors, such as myogenin, MRF4, Myf5 or MyoD, presumably because these are expresser at low levels below the detection limits of the LC-MS methodology used here. Previous proteomic studies of the myogenic differentiation program using 2D-PAGE-based technology have likewise failed to identify these factors (11), indicating an important limitation of proteomic profiling using current instrumentation.

Nonetheless, several other developmentally important transcriptional regulators were identified in this analysis (**Table 4**), including the homeobox proteins Six 1 and Six 4, whose levels were sharply elevated immediately following serum withdrawal, consistent with previous reports (40). Both factors have been implicated in the control of muscle formation through binding to an evolutionary conserved MEF3-binding site upstream of the myogenin promoter and resulting in the activation of myogenin transcription (40), a key step in skeletal muscle development. The MEF3 site is also present in other skeletal muscle-specific genes, including the promoters of genes encoding troponin C (41), creatine kinase (42), and the glycolytic enzyme aldolase A (43,44), all of which were detected as being up-regulated during later stages of myogenic differentiation. Likewise, myocyte nuclear factor (MNF, also known as Forkhead box protein K1) was also detected immediately following serum deprivation (**Supplementary Table S4**), consistent with an early role in myogenic differentiation (45,46). MNF encodes one of the first winged-helix HNF-3/fork head family of transcription factors identified as a key regulator of the myogenic program (46,47). It acts by binding to the CCAC-box sequence motif found in the promoter region of the myoglobin gene and thereby activating transcription (45).

Intracellular mediators of myogenic signaling

Although a crude nuclear preparation (expected to contain nuclear, contractile and mitochondrial proteins) was prepared, we were also able to detect a diverse set of proteins involved in signal transduction (see **Supplementary Table S4** for details). In particular, key members of the Ras superfamily of signaling proteins, which broadcast a host of signals from activated receptor tyrosine kinases at the cell surface through to the nucleus (48,49), were identified, particularly during the initial stages of cell differentiation. For instance, elevated levels of both R-Ras and the Ras-related protein Rab-33B, were detected immediately following serum withdrawal. Likewise,

several critical downstream targets of Ras were induced at early stages of differentiation, including the mitogen-activated protein kinases MAPKK-1 and -2, ERK-1 and the MAPKK1-interacting protein 1, as well as AF-6, a putative signaling protein. In contrast, the Ras GTPase-activating-like protein IQRAP1, which is proposed to participate in the reorganization of the actin cytoskeleton during cellular remodeling (50), was found to be expressed throughout all stages of myogenesis was detected exclusively in the proliferating myoblasts. Taken together, these data indicate that significant differences in the accumulation of core components of RAS-MAPK mediated signaling occur during the myogenic process.

In contrast, components of at least two major signaling pathways known to inhibit myogenic differentiation were found to be down-regulated in response to initiation of myogenic program (**Tables 2** and **3**). The first major pathway involves Notch signaling, which inhibits myogenesis by interfering with MEF2 activation (51-53). For instance, Notch 3, and 4 were detected preferentially in the proliferating myoblasts (Day 2), consistent with the results of previous microarray studies (6). The second pathway involves the SMAD family of signaling proteins (54,55). The transcription factors SMAD3, -4 and -5, were all detected preferentially early during myogenesis (i.e., in proliferating myoblasts and early-stage myotubes), again consistent with a proliferative function.

Several other notable signaling factors (**Supplementary Table S4**) were preferentially detected in the late-stage myotubes, including ArgBP2, DCAMKL1 and Copine III. ArgBP2 is a novel member of the Abelson (Arg/Abl) protein-tyrosine kinase-binding proteins, and is predicted to be a substrate of Arg and v-Abl (56). ArgBP2 localizes to the Z-disc in cardiac muscle, where it likely influences contractility and elastic properties of cardiac sarcomeres in response to activation of Abelson-linked signaling cascades (56). DCAMKL1 is a serine/threonine protein kinase implicated in Ca^{2+} signaling, and has been shown to control neuronal cell migration in the

developing brain (57). On the other hand, Copine III, a putative protein kinase detected in both proliferating and early differentiating cells, has been linked to the regulation of membrane trafficking (58).

Sarcomeric organization and muscle contraction

Myofibrils, which form the bulk of muscle mass, are composed of tandem arrays of sarcomeres, the core structural unit of dynamically interacting chains of actin and myosin filaments responsible for muscle contraction (59). The development and maturation of the contractile apparatus requires a parallel increase in calcium-dependent cycling proteins to handle the rapid fluxes in Ca^{2+}-associated with muscle contractility (60). Consistent with this, myotube formation was associated with elevated levels of calcium-transporters, including the Ca^{2+} release channel (ryanodine receptor, RyR), voltage-gated L-type calcium channel, and the sarco(endo)plasmic reticulum calcium ATPase (SERCA). As expected, a large set of other proteins linked to skeletal muscle ***excitation/contraction*** (such as the cytoskeletal factors actin, myosin, troponin, nebulin, titin, desmin and α-actinin) were likewise enriched in late stage differentiating cells (**Table 4** and **Supplementary Table S8**).

The ATP requirements of contracting muscle are extremely high, both for ATP-dependent Ca^{2+} handling and for ATP-dependent myosin cross-bridge formation. As a result of this marked demand, skeletal muscle metabolizes large amounts of glucose, fatty acids and amino acids to fuel contraction (61). Consistent with this, late stage myotubes were greatly enriched in enzymes linked to basic metabolism, including key rate-limiting energy producing enzymes such as pyruvate kinase, creatine kinase, ATP synthase, acyl-coenzyme A oxidases, and 3-hydroxyacyl-CoA dehydrogenases (**Table 6** and **Supplementary Table S10**).

Cytoskeleton and extracellular matrix reorganization

The muscle cytoskeleton consists of a complex network of filaments and tubules that transmit mechanical and chemical stimuli within and between adjacent myocytes. This dynamic structure also contributes to cell stability during the contraction cycle by anchoring subcellular structures such as mitochondria, nuclei and myofibrils. The stabilizing mechano-transducer action is supported by membrane-associated proteins, in particular dystrophin, which binds to intracellular actin and extracellular laminin through the dystroglycan complex (62). As expected, myogenesis was associated with the induction of a vast array of cytoskeletal factors, such as desmin and nebulin, as well as muscle-specific components of the dystrophin complex, such as dystroglycan and sarcoglycan.

Reorganization of the contractile apparatus was paralleled by an increased abundance of connective tissue proteins in the developing myocytes, which provide physical stabilization during the extreme tensile forces generated during contraction. These included numerous collagen α isoforms, integrins (α-5, α-v, α-7, β-1, β-5), laminins (α-2, α-5, β-1, γ-1), and fibronectin. In addition, matrix metalloproteases, including glycoproteins, and adhesion factors, such as α- and β-sarcoglycan, were expressed preferentially during cell differentiation, or were detected exclusively in terminally differentiated myotubes. Numerous other adhesion or structural proteins, including nidogen, and dystroglycan, were also enriched in later stages of differentiation.

Protein functional annotation

In this study, we detected expression of ~25 uncharacterized RIKEN cDNAs and ~180 putative "hypothetical" proteins. Comparison of their expression profiles to those of previously studied proteins can provide clues as to the possible functions or roles of these gene products. In particular, linkage to a specific cluster exhibiting significant functional enrichment suggests that

several of these uncharacterized proteins are likely to participate in processes important to proper myogenesis, including the control of mRNA transcription, chromatin modification, and/or cell cycle progression.

Of course, the observed clusters of functionally-related proteins highlighted in this report reflect only a portion of all the proteins identified in this study. In addition to suggesting a potential role for novel gene products in skeletal muscle development, our results implicate a number of well characterized proteins that have not previously been linked to muscle cell differentiation. For example, two proteins involved in RNA synthesis (ATP-dependent RNA helicase [DEAD-box protein] and UMP/CMP kinase) as well as a protein involved in endocytosis (intersectin-1) were found to be differentially expressed during myogenic differentiation, yet these proteins had not been associated with muscle development previously. A systematic, hypothesis-driven analysis of similarly identified proteins based on reasonable interpretations of their expression characteristics seems likely to bear fruit. Hence, our proteomic data can be viewed as a resource for targeted follow up studies centered on one or more biochemical pathways of particular interest.

Comparison to microarray-based investigations of myogenic gene transcription

In the past year, several studies have reported the use of DNA microarray technology to probe changes in gene expression in C2C12 cells coincident with the formation of mature myocytes (5-7). Gratifyingly, the results of the most extensive gene expression study published to date (7) were found to correlate quite well with the proteomic data reported here, with relatively few substantive inconsistencies, at least in terms of overall temporal trends. This concordance was somewhat surprisingly given the general feeling in the field, and validates the general conclusions of the two studies and the respective experimental platforms and further encourages follow-up investigations. Hence, while gene expression profiling studies generally achieved a more extensive

coverage (at least 2,895 mRNA transcripts were predicted to be expressed throughout skeletal myogenesis in ref. (7), our study provides a complementary evidence for possible post-translational controls that may serve to further refine the biochemical transitions associated with myogenesis. Moreover, while certain of gross incongruities in the observed patterns of protein and transcript levels are likely to have arisen due to technical limitations, such as biased detection or other artifacts associated with LC-MS and microarray analyses, many may in fact represent bone fide, biologically-meaningful differences, stemming from differential regulation of translation and/or mRNA or protein stability, as has also been previously suggested in the literature (63).

Comparison to 2D-PAGE profiling of myogenesis

A recent study (11) reported the use of 2D-PAGE, followed by silver staining and quantitative imaging, to examine changes in the levels of ~2,000 protein spots throughout the myogenic differentiation. Although the vast majority did not exhibit any detectable differences in terms of relative abundance, ~100 predicted to be differentially expressed were identified, including some 26 phosphorylated variants. We determined that there were 39 proteins in total that were detected in the Tannu paper as well as this study (using an 85%+ confidence filter); 29 of which (74%) showed virtually identical findings (see **Supplementary Table S11** for details), whereas only 10 (26%) proteins (annexin V, protein disulfide isomerase, transcription intermediary factor 1-beta, histone acetyl transferase type B, guanine nucleotide binding protein beta subunit, 26S proteasome regulatory subunit, Lasp-1, 75 kD glucose regulated protein, secreted protein acidic and rich in cysteine (SPARC), and myosin light chain 1) showed significant differences in expression patterns between the two studies.

These modest discrepancies most likely arose due to technical differences in tissue culture, protein extraction or sample preparation. Although gel-based profiling techniques offer certain

advantages (65), this study indicates that gel-free shotgun methods offer fundamentally enhanced proteomic coverage (14). Nevertheless, despite the limited dynamic range afforded by SDS-PAGE, the substantial agreement between these two independent proteomic datasets further validates the main conclusions of this new study and the reliability of gel-free protein expression profiling as a means to investigate fundamental aspects of muscle cell biology.

Figure legends

Figure 1. Gross changes in cell morphology in response to myogenic differentiation. Light microscopy-based images of undifferentiated (day 0) proliferating C2C12 myoblasts (*MB*) and differentiating cells at various time-points (days 2, 4 and 6) following serum starvation and induction of the myogenic program. Bar, 450 μm.

Figure 2. Hierarchical clustering of the myogenic proteomic profiles. For this time-course analysis, relative protein abundance was calculated based on the ratio of the natural logarithm of the protein spectral count detected in each of the differentiation time-points (2-10 days post serum withdrawal) relative to that observed in the proliferating myoblast cell population (*MB*; i.e., day 0). Cluster membership was evaluated for statistical enrichment to select functional annotation categories (GO-terms) in order to reveal biologically-relevant changes in the underlying patterns of protein expression. A few select, statistically significant GO terms are reported. Symbols: *MB*, myoblast; *MT*, myotubes; *Ref*., reference sample.

Figure 3. Independent validation of the differential expression patterns of select transcription factors by RT-PCR. Fluctuations in mRNA transcript levels of select transcription factors throughout the differentiation program were assessed using RT-PCR. The inlaid values represent the corresponding proteomic spectral counts detected in the corresponding protein fractions.

Figure 4. Comparison of the proteomic profiles to a recently published myogenic gene expression dataset. Comparison of the proteomic profiles to a recently published DNA microarray-based analysis of gene expression throughout a similar myogenic time-course by Tomczak *et al.* (7). 547 pairs of cognate protein-mRNA transcripts were cross-referenced. The

datasets were then combined, normalized, and co-clustered, and a heat map was generated. Concordant co-expression was observed for mRNA transcripts normalized to the probe signal levels detected in either day –2 [374 protein – gene pairs] (**A**) or day 0 [123 protein – gene pairs] (**B**) samples using the Tomczak *et al.* nomenclature (7). Individual clusters were exported and analyzed for significantly enriched GO-terms. Statistically-significantly ($10e^{-5}$) functional categories are displayed next to each cluster. Discordant expression patterns were observed for a subset of the gene products [50 protein – gene pairs] (**C**), using either day -2 (not shown) or day 0 (shown here) normalized microarray data.

Table legends

Table 1. High confidence proteins identified by mass spectrometry. Listed are the total number of proteins and corresponding spectral counts identified in each cell fraction.

Table 2. Functional assessment of myoblast specific proteins. Representative proteins detected exclusively in the starting mitotic undifferentiated myoblast cell population (*MB*; day 0) that map to statistically-enriched functional categories. The respective GO-terms, corresponding SwissProt/TrEMBL locus IDs, protein descriptions and number of detected spectra are reported. (*MB*, proliferating myoblast precursors; *2-10d*, differentiation time-points).

Table 3. Proteins up-regulated during early-stage differentiation (Day 2 specific). Representative proteins mapping to significantly-enriched functional categories (GO-terms) up-regulated in early-stage (Day 2) differentiating cells as compared to the myoblast precursor cell population (MB) or later time points.

Table 4. Proteins up-regulated in response to myogenic differentiation. Representative proteins mapping to discrete functional categories significantly up-regulated during myotube formation (days 2-10) as compared to undifferentiated myoblasts.

Table 5. Proteins down-regulated in response to exit from the cell cycle and terminal differentiation. Representative proteins mapping to functional categories substantially down-regulated in differentiating myotubes (Days 2-10) as compared to proliferating myoblasts.

Table 6. Proteins up-regulated in late-stage, fully differentiated myotubes. Significantly-enriched GO-term categories associated with proteins detected uniquely in fully differentiated (i.e., functional) myotubes (day 10).

Acknowledgements

A.O.G. and Y.P. were Postdoctoral Research Fellows of the Heart and Stroke Foundation of Canada and Ontario, respectively. This research was supported by Canadian Institutes of Health Research grant #MOP 49493 and the Neuromuscular Research Partnership and a grant from the Muscular Dystrophy Association (USA) to D.H.M.; and by a developmental grant from the Muscular Dystrophy Association (USA) to A.O.G. and by grants from the Natural Sciences and Engineering Research Council of Canada, the Protein Engineering Network Centre of Excellence (PENCE) and funds from the Ontario Genome Institute and Genome Canada to A.E.

References

1. Pownall, M. E., Gustafsson, M. K., and Emerson, C. P., Jr. (2002) Myogenic regulatory factors and the specification of muscle progenitors in vertebrate embryos. *Annu Rev Cell Dev Biol* 18, 747-783
2. Parker, M. H., Seale, P., and Rudnicki, M. A. (2003) Looking back to the embryo: defining transcriptional networks in adult myogenesis. *Nat Rev Genet* 4, 497-507
3. Arnold, H. H., and Winter, B. (1998) Muscle differentiation: more complexity to the network of myogenic regulators. *Curr Opin Genet Dev* 8, 539-544
4. Black, B. L., and Olson, E. N. (1998) Transcriptional control of muscle development by myocyte enhancer factor-2 (MEF2) proteins. *Annu Rev Cell Dev Biol* 14, 167-196
5. Shen, X., Collier, J. M., Hlaing, M.*, et al.* (2003) Genome-wide examination of myoblast cell cycle withdrawal during differentiation. *Dev Dyn* 226, 128-138
6. Delgado, I., Huang, X., Jones, S.*, et al.* (2003) Dynamic gene expression during the onset of myoblast differentiation in vitro. *Genomics* 82, 109-121
7. Tomczak, K. K., Marinescu, V. D., Ramoni, M. F.*, et al.* (2004) Expression profiling and identification of novel genes involved in myogenic differentiation. *Faseb J* 18, 403-405
8. Gygi, S. P., Rochon, Y., Franza, B. R.*, et al.* (1999) Correlation between protein and mRNA abundance in yeast. *Mol Cell Biol* 19, 1720-1730
9. Greenbaum, D., Colangelo, C., Williams, K.*, et al.* (2003) Comparing protein abundance and mRNA expression levels on a genomic scale. *Genome Biol* 4, 117
10. Hegde, P. S., White, I. R., and Debouck, C. (2003) Interplay of transcriptomics and proteomics. *Curr Opin Biotechnol* 14, 647-651
11. Tannu, N. S., Rao, V. K., Chaudhary, R. M.*, et al.* (2004) Comparative proteomes of the proliferating C2C12 myoblasts and fully differentiated myotubes reveal the complexity of the skeletal muscle differentiation program. *Mol Cell Proteomics*
12. Griffin, T. J., Goodlett, D. R., and Aebersold, R. (2001) Advances in proteome analysis by mass spectrometry. *Curr Opin Biotechnol* 12, 607-612
13. Gygi, S. P., Rist, B., and Aebersold, R. (2000) Measuring gene expression by quantitative proteome analysis. *Curr Opin Biotechnol* 11, 396-401
14. Kislinger, T., and Emili, A. (2003) Going global: protein expression profiling using shotgun mass spectrometry. *Curr Opin Mol Ther* 5, 285-293
15. Aebersold, R., and Mann, M. (2003) Mass spectrometry-based proteomics. *Nature* 422, 198-207
16. Washburn, M. P., Wolters, D., and Yates, J. R., 3rd. (2001) Large-scale analysis of the yeast proteome by multidimensional protein identification technology. *Nat Biotechnol* 19, 242-247
17. Kislinger, T., Rahman, K., Radulovic, D.*, et al.* (2003) PRISM, a Generic Large Scale Proteomic Investigation Strategy for Mammals. *Mol Cell Proteomics* 2, 96-106
18. Eng, J. K., McCormack, A. L., and Yates, J. R. I. (1994) An approach to correlate tandem mass-spectral data of peptides with amino-acid-sequences in a protein database. *J Am Soc Mass Spectrom* 11, 976-989
19. Ashburner, M., Ball, C. A., Blake, J. A.*, et al.* (2000) Gene ontology: tool for the unification of biology. The Gene Ontology Consortium. *Nat Genet* 25, 25-29
20. Liu, H., Sadygov, R. G., and Yates, J. R., 3rd. (2004) A model for random sampling and estimation of relative protein abundance in shotgun proteomics. *Anal Chem* 76, 4193-4201

21. Eisen, M. B., Spellman, P. T., Brown, P. O.*, et al.* (1998) Cluster analysis and display of genome-wide expression patterns. *Proc Natl Acad Sci U S A* 95, 14863-14868
22. Robinson, M. D., Grigull, J., Mohammad, N.*, et al.* (2002) FunSpec: a web-based cluster interpreter for yeast. *BMC Bioinformatics* 3, 35
23. Gramolini, A. O., and Jasmin, B. J. (1999) Expression of the utrophin gene during myogenic differentiation. *Nucleic Acids Res* 27, 3603-3609
24. Corthals, G. L., Wasinger, V. C., Hochstrasser, D. F.*, et al.* (2000) The dynamic range of protein expression: a challenge for proteomic research. *Electrophoresis* 21, 1104-1115
25. Bairoch, A., and Apweiler, R. (2000) The SWISS-PROT protein sequence database and its supplement TrEMBL in 2000. *Nucleic Acids Res* 28, 45-48
26. Wu, L. F., Hughes, T. R., Davierwala, A. P.*, et al.* (2002) Large-scale prediction of Saccharomyces cerevisiae gene function using overlapping transcriptional clusters. *Nat Genet* 31, 255-265
27. Rida, P. C., Le Minh, N., and Jiang, Y. J. (2004) A Notch feeling of somite segmentation and beyond. *Dev Biol* 265, 2-22
28. Sheffield-Moore, M., and Urban, R. J. (2004) An overview of the endocrinology of skeletal muscle. *Trends Endocrinol Metab* 15, 110-115
29. Guttridge, D. C. (2004) Signaling pathways weigh in on decisions to make or break skeletal muscle. *Curr Opin Clin Nutr Metab Care* 7, 443-450
30. Le Roch, K. G., Johnson, J. R., Florens, L.*, et al.* (2004) Global analysis of transcript and protein levels across the Plasmodium falciparum life cycle. *Genome Res* 14, 2308-2318
31. Schulz, R. A., and Yutzey, K. E. (2004) Calcineurin signaling and NFAT activation in cardiovascular and skeletal muscle development. *Dev Biol* 266, 1-16
32. Martin, P. T. (2003) Role of transcription factors in skeletal muscle and the potential for pharmacological manipulation. *Curr Opin Pharmacol* 3, 300-308
33. Solloway, M. J., and Harvey, R. P. (2003) Molecular pathways in myocardial development: a stem cell perspective. *Cardiovasc Res* 58, 264-277
34. Baylies, M. K., and Michelson, A. M. (2001) Invertebrate myogenesis: looking back to the future of muscle development. *Curr Opin Genet Dev* 11, 431-439
35. Walsh, K., and Perlman, H. (1997) Cell cycle exit upon myogenic differentiation. *Curr Opin Genet Dev* 7, 597-602
36. Wei, Q., and Paterson, B. M. (2001) Regulation of MyoD function in the dividing myoblast. *FEBS Lett* 490, 171-178
37. Puri, P. L., and Sartorelli, V. (2000) Regulation of muscle regulatory factors by DNA-binding, interacting proteins, and post-transcriptional modifications. *J Cell Physiol* 185, 155-173
38. Ornatsky, O. I., and McDermott, J. C. (1996) MEF2 protein expression, DNA binding specificity and complex composition, and transcriptional activity in muscle and non-muscle cells. *J Biol Chem* 271, 24927-24933
39. Di Lisi, R., Millino, C., Calabria, E.*, et al.* (1998) Combinatorial cis-acting elements control tissue-specific activation of the cardiac troponin I gene in vitro and in vivo. *J Biol Chem* 273, 25371-25380
40. Spitz, F., Demignon, J., Porteu, A.*, et al.* (1998) Expression of myogenin during embryogenesis is controlled by Six/sine oculis homeoproteins through a conserved MEF3 binding site. *Proc Natl Acad Sci U S A* 95, 14220-14225
41. Parmacek, M. S., Ip, H. S., Jung, F.*, et al.* (1994) A novel myogenic regulatory circuit controls slow/cardiac troponin C gene transcription in skeletal muscle. *Mol Cell Biol* 14, 1870-1885

42. Himeda, C. L., Ranish, J. A., Angello, J. C., *et al.* (2004) Quantitative proteomic identification of six4 as the trex-binding factor in the muscle creatine kinase enhancer. *Mol Cell Biol* 24, 2132-2143
43. Joh, K., Takano, K., Mukai, T., *et al.* (1991) Analysis of upstream regulatory regions required for the activities of two promoters of the rat aldolase A gene. *FEBS Lett* 292, 128-132
44. Spitz, F., Salminen, M., Demignon, J., *et al.* (1997) A combination of MEF3 and NFI proteins activates transcription in a subset of fast-twitch muscles. *Mol Cell Biol* 17, 656-666
45. Bassel-Duby, R., Hernandez, M. D., Yang, Q., *et al.* (1994) Myocyte nuclear factor, a novel winged-helix transcription factor under both developmental and neural regulation in striated myocytes. *Mol Cell Biol* 14, 4596-4605
46. Yang, Q., Bassel-Duby, R., and Williams, R. S. (1997) Transient expression of a winged-helix protein, MNF-beta, during myogenesis. *Mol Cell Biol* 17, 5236-5243
47. Lai, E., Clark, K. L., Burley, S. K., *et al.* (1993) Hepatocyte nuclear factor 3/fork head or "winged helix" proteins: a family of transcription factors of diverse biologic function. *Proc Natl Acad Sci U S A* 90, 10421-10423
48. Scita, G., Tenca, P., Frittoli, E., *et al.* (2000) Signaling from Ras to Rac and beyond: not just a matter of GEFs. *Embo J* 19, 2393-2398
49. Molkentin, J. D., and Dorn, I. G., 2nd. (2001) Cytoplasmic signaling pathways that regulate cardiac hypertrophy. *Annu Rev Physiol* 63, 391-426
50. Presslauer, S., Hinterhuber, G., Cauza, K., *et al.* (2003) RasGAP-like protein IQGAP1 is expressed by human keratinocytes and recognized by autoantibodies in association with bullous skin disease. *J Invest Dermatol* 120, 365-371
51. Dahlqvist, C., Blokzijl, A., Chapman, G., *et al.* (2003) Functional Notch signaling is required for BMP4-induced inhibition of myogenic differentiation. *Development* 130, 6089-6099
52. Wilson-Rawls, J., Molkentin, J. D., Black, B. L., *et al.* (1999) Activated notch inhibits myogenic activity of the MADS-Box transcription factor myocyte enhancer factor 2C. *Mol Cell Biol* 19, 2853-2862
53. Conboy, I. M., and Rando, T. A. (2002) The regulation of Notch signaling controls satellite cell activation and cell fate determination in postnatal myogenesis. *Dev Cell* 3, 397-409
54. Zhu, S., Goldschmidt-Clermont, P. J., and Dong, C. (2004) Transforming growth factor-beta-induced inhibition of myogenesis is mediated through Smad pathway and is modulated by microtubule dynamic stability. *Circ Res* 94, 617-625
55. Yamamoto, N., Akiyama, S., Katagiri, T., *et al.* (1997) Smad1 and smad5 act downstream of intracellular signalings of BMP-2 that inhibits myogenic differentiation and induces osteoblast differentiation in C2C12 myoblasts. *Biochem Biophys Res Commun* 238, 574-580
56. Moresco, E. M., and Koleske, A. J. (2003) Regulation of neuronal morphogenesis and synaptic function by Abl family kinases. *Curr Opin Neurobiol* 13, 535-544
57. Burgess, H. A., and Reiner, O. (2000) Doublecortin-like kinase is associated with microtubules in neuronal growth cones. *Mol Cell Neurosci* 16, 529-541
58. Caudell, E. G., Caudell, J. J., Tang, C. H., *et al.* (2000) Characterization of human copine III as a phosphoprotein with associated kinase activity. *Biochemistry* 39, 13034-13043
59. Clark, K. A., McElhinny, A. S., Beckerle, M. C., *et al.* (2002) Striated muscle cytoarchitecture: an intricate web of form and function. *Annu Rev Cell Dev Biol* 18, 637-706
60. MacLennan, D. H., and Kranias, E. G. (2003) Phospholamban: a crucial regulator of cardiac contractility. *Nat Rev Mol Cell Biol* 4, 566-577

61. Sartorelli, V., and Fulco, M. (2004) Molecular and cellular determinants of skeletal muscle atrophy and hypertrophy. *Sci STKE* 2004, re11
62. Lapidos, K. A., Kakkar, R., and McNally, E. M. (2004) The dystrophin glycoprotein complex: signaling strength and integrity for the sarcolemma. *Circ Res* 94, 1023-1031
63. Tian, Q., Stepaniants, S. B., Mao, M.*, et al.* (2004) Integrated Genomic and Proteomic Analyses of Gene Expression in Mammalian Cells. *Mol Cell Proteomics* 3, 960-969
64. Koller, A., Washburn, M. P., Lange, B. M.*, et al.* (2002) Proteomic survey of metabolic pathways in rice. *Proc Natl Acad Sci U S A* 99, 11969-11974

Figures

Figure 1

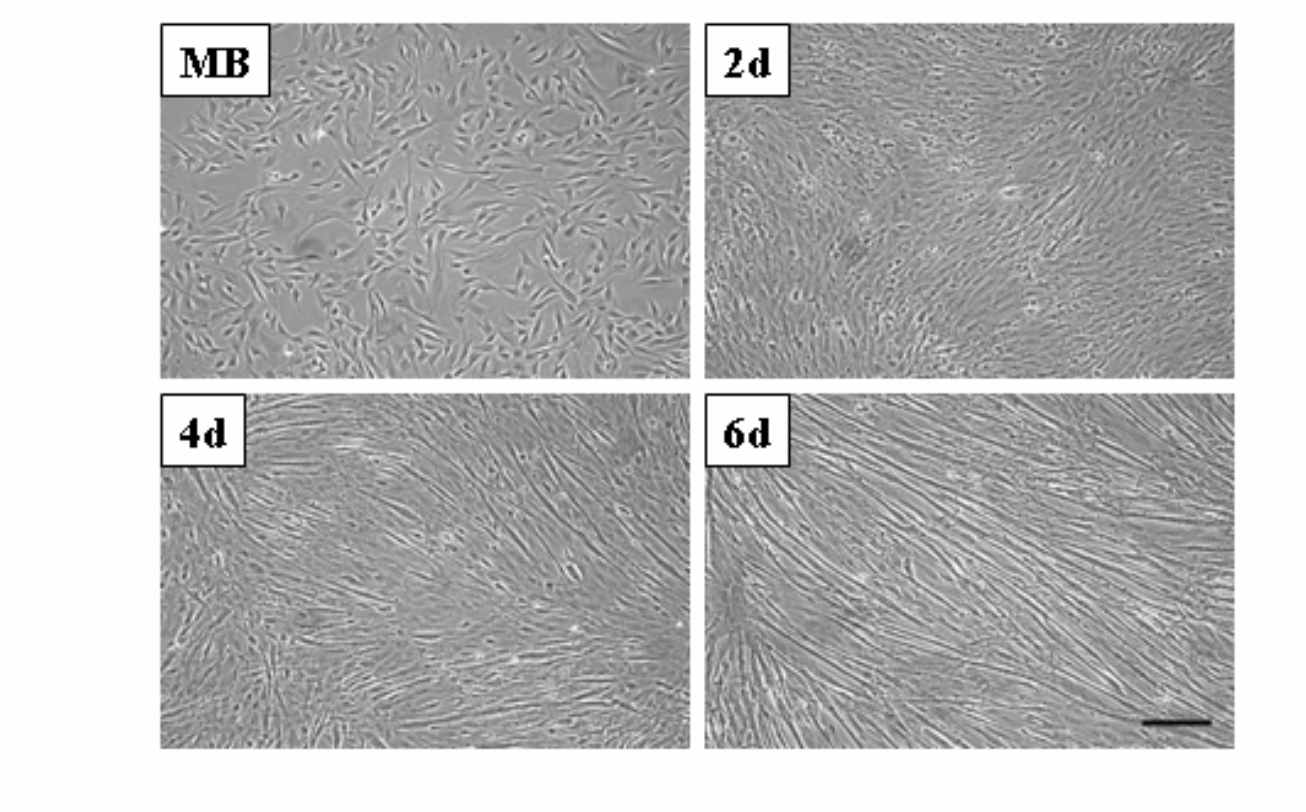

Figure 2

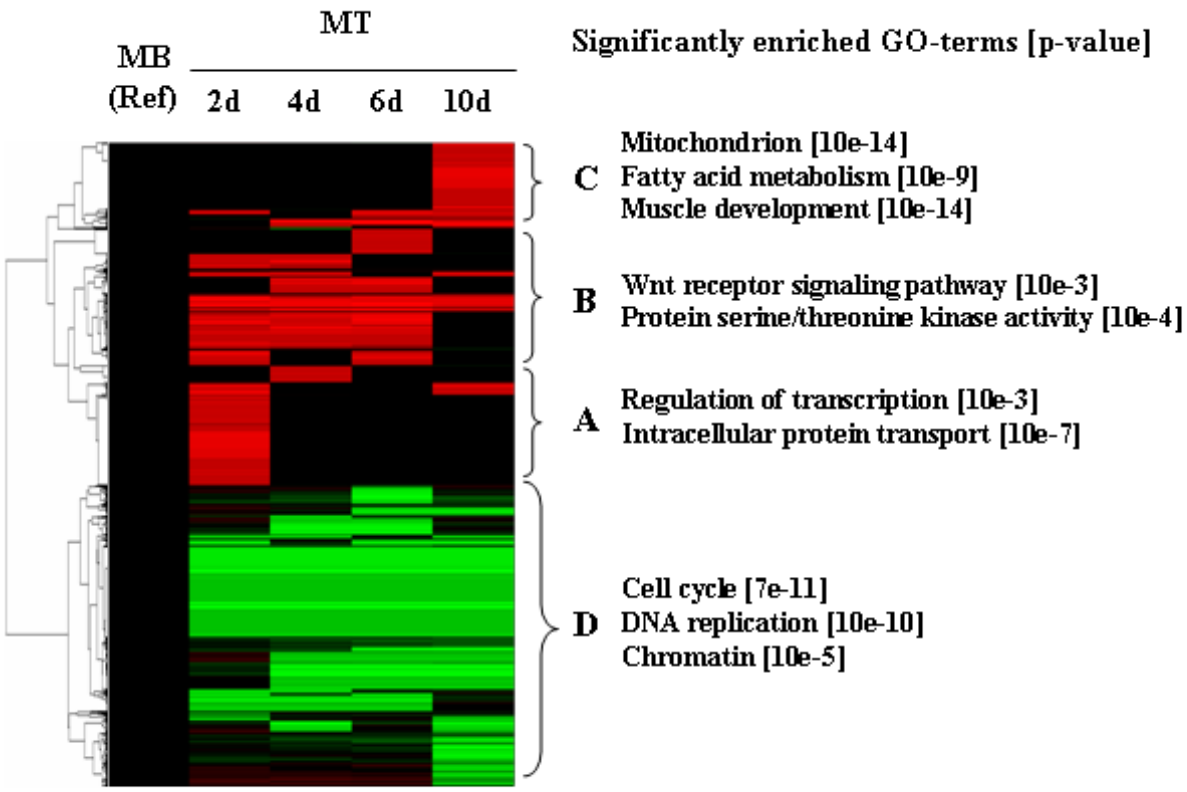

Figure 3

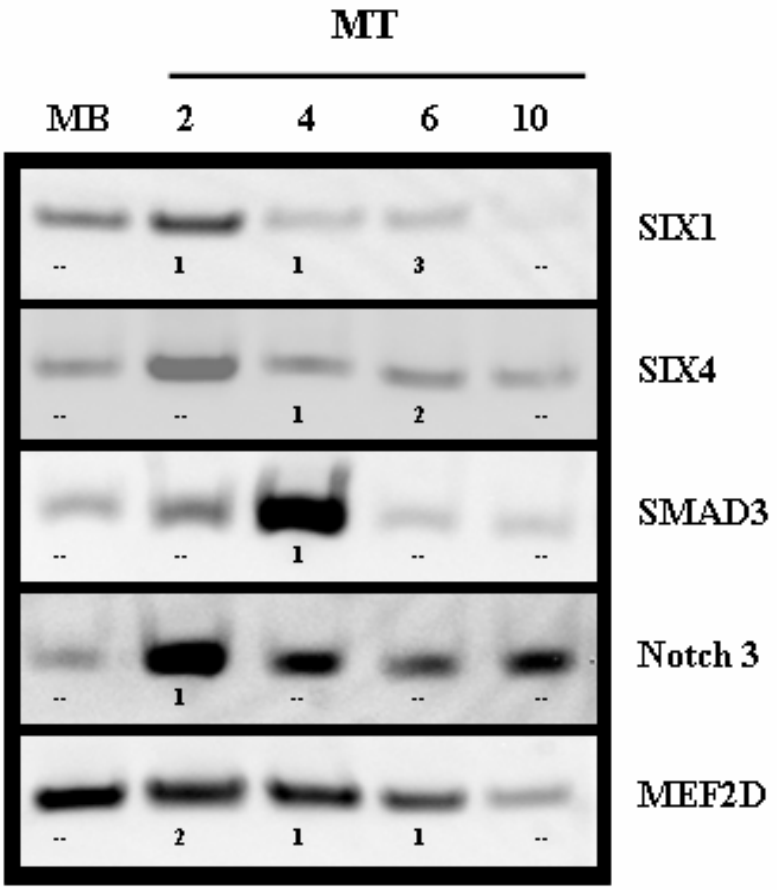

Figure 4

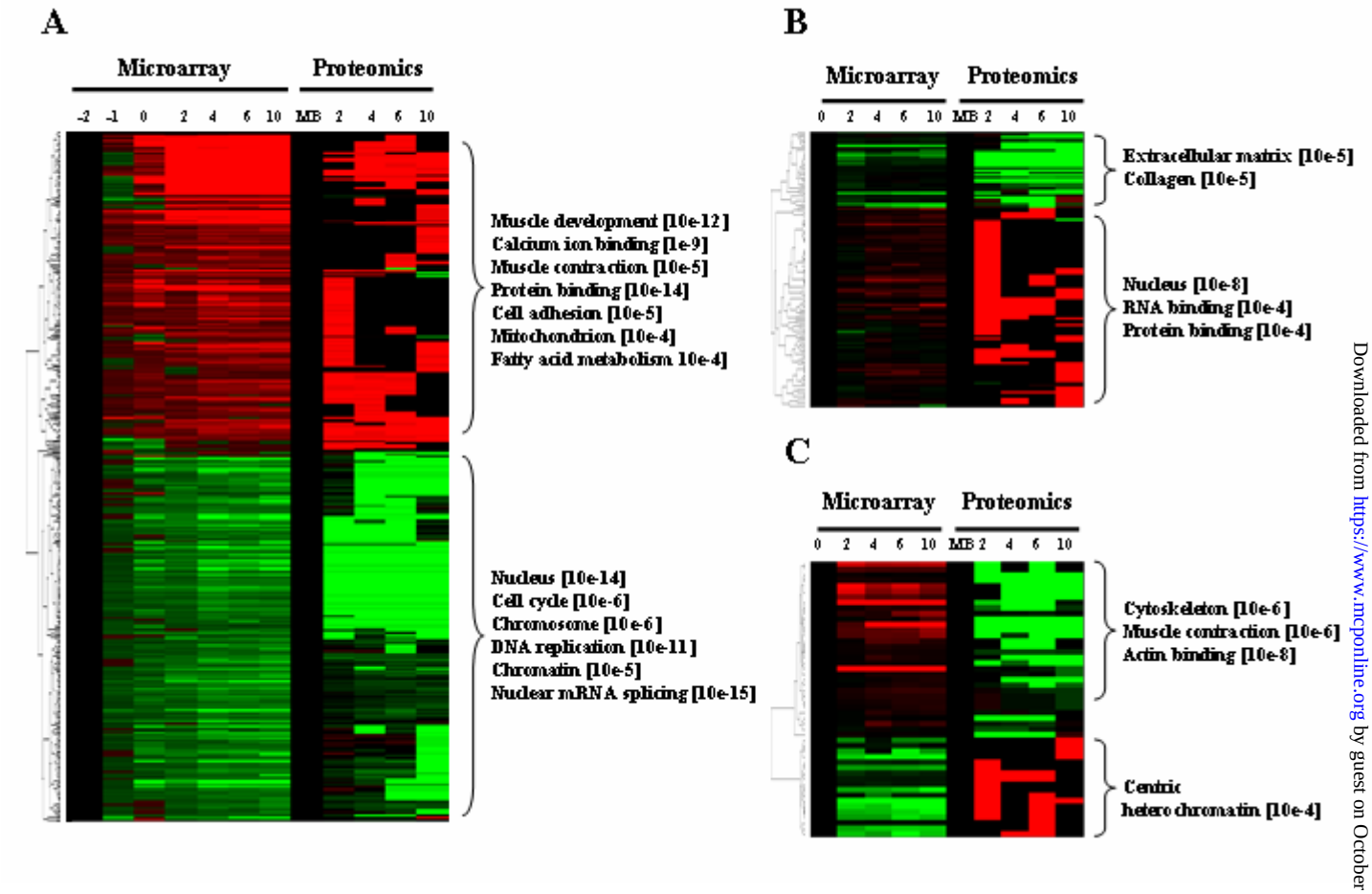

Tables

Table 1:

Time-point	proteins	total spectral count
MB	946	6550
Day 2	1128	6478
Day 4	749	4723
Day 6	735	4194
Day 10	709	3165
Total	1865	25110
reverse (%)	43 (2.3%)	90 (0.36%)

Table 2:

Functional categories [GO-terms] Proteins identified	MB	2d	4d	6d	10d	Description
nucleus [GO:0005634]						
CBP_MOUSE	2	--	--	--	--	CREB-binding protein
CUL3_MOUSE	2	--	--	--	--	Cullin homolog 3
DPO2_MOUSE	1	--	--	--	--	DNA polymerase alpha 70 kDa subunit
NPL1_MOUSE	4	--	--	--	--	Nucleosome assembly protein 1-like 1
cell cycle [GO:0007049]						
CKS1_HUMAN	2	--	--	--	--	Cyclin-dependent kinases regulatory subunit 1
CUL3_MOUSE	2	--	--	--	--	Cullin homolog 3
DNA replication [GO:0006260]						
CAFA_MOUSE	1	--	--	--	--	Chromatin assembly factor 1 subunit A
MCM4_MOUSE	2	--	--	--	--	DNA replication licensing factor MCM4
PRI2_MOUSE	1	--	--	--	--	DNA primase large subunit
RFA2_MOUSE	2	--	--	--	--	Replication protein A 32 kDa subunit
chromosome [GO:0005694]						
HMG4_MOUSE	1	--	--	--	--	High mobility group protein 4
PR4B_MOUSE	1	--	--	--	--	Serine/threonine-protein kinase PRP4 homolog
TRF2_MOUSE	1	--	--	--	--	Telomeric repeat binding factor 2
DNA binding [GO:0003677]						
HCC1_MOUSE	3	--	--	--	--	Nuclear protein Hcc-1
KF4A_MOUSE	3	--	--	--	--	Chromosome-associated kinesin KIF4A
RB56_HUMAN	2	--	--	--	--	TATA-binding protein associated factor 2N
protein biosynthesis [GO:0006412]						
IF37_MOUSE	5	--	--	--	--	Eukaryotic translation initiation factor 3 subunit 7
Q62448	1	--	--	--	--	Eukaryotic translation initiation factor 4 gamma 2
Q8R3M7	3	--	--	--	--	Similar to eukaryotic translation initiation factor 3, subunit
R35A_MOUSE	1	--	--	--	--	60S ribosomal protein L35a
RL32_HUMAN	3	--	--	--	--	60S ribosomal protein L32
MCA1_MOUSE	1	--	--	--	--	Multisynthetase complex auxiliary component p43
cytoskeleton [GO:0005856]						
ACTZ_HUMAN	6	--	--	--	--	Alpha-centractin (Centractin)
DCT2_MOUSE	2	--	--	--	--	Dynactin complex 50 kDa subunit
PRO1_MOUSE	1	--	--	--	--	Profilin I

Table 3:

Functional categories [GO-terms] Proteins identified	MB	2d	4d	6d	10d	Description
nucleus [GO:0005634]						
CGBP_MOUSE	--	1	--	--	--	CpG binding protein
VDR_MOUSE	--	1	--	--	--	Vitamin D3 receptor
FM14_MOUSE	--	1	--	--	--	Formin 1 isoform IV
Q91ZW3	--	3	--	--	--	ATP-dependent chromatin remodeling protein SNF2H
regulation of transcription [GO:0006355]						
O54978	--	10	--	--	--	Zince finger protein
KLF4_MOUSE	--	1	--	--	--	Kruppel-like factor 4
MEI1_MOUSE	--	1	--	--	--	Homeobox protein Meis1
NCR1_MOUSE	--	5	--	--	--	Nuclear receptor co-repressor 1
FZD2_MOUSE	--	1	--	--	--	Frizzled 2 precursor
SMA4_MOUSE	--	1	--	--	--	Mothers against decapentaplegic homolog 4 (SMAD 4)
Q96ME7	--	9	--	--	--	Zinc finger protein 512
Q8VDM0	--	2	--	--	--	Similar to lamin B receptor
protein binding [GO:0005515]						
NTC3_MOUSE	--	3	--	--	--	Neurogenic locus notch homolog protein 3 precursor
STX4_MOUSE	--	1	--	--	--	Syntaxin 4
Q99MI2	--	3	--	--	--	Rab6-interacting protein 2 isoform A
MY5A_MOUSE	--	2	--	--	--	Myosin 5
TRIA_HUMAN	--	2	--	--	--	Thyroid receptor interacting protein

Table 4:

Functional categories [GO-terms] Proteins identified	MB	2d	4d	6d	10d	Description
nucleus [GO:0005634]						
DD19_MOUSE	--	2	1	2	--	ATP-dependent RNA helicase DDX19
EMD_MOUSE	--	--	--	--	1	Emerin
GABB_MOUSE	--	1	2	--	--	GA binding protein beta-1 chain
HTF4_MOUSE	--	2	1	1	--	Transcription factor 12
ITF2_MOUSE	--	--	--	1	--	Transcription factor 4
LAM1_MOUSE	--	--	--	--	3	Lamin B1
SIX1_MOUSE	--	1	1	3	--	Homeobox protein SIX1
SIX4_MOUSE	--	--	1	2	--	Homeobox protein SIX4
mitochondrion [GO:0005739]						
ACDL_MOUSE	--	--	--	--	3	Acyl-CoA dehydrogenase, long-chain specific
ACDS_MOUSE	--	--	--	--	2	Acyl-CoA dehydrogenase, short-chain specific
ACDV_MOUSE	--	--	--	--	1	Acyl-CoA dehydrogenase, very-long-chain specific
ATPA_MOUSE	1	5	3	8	17	ATP synthase alpha chain
ATPB_MOUSE	5	8	7	31	59	ATP synthase beta chain
ATPD_MOUSE	--	--	--	--	7	ATP synthase D chain
ATPG_MOUSE	--	--	--	--	3	ATP synthase gamma chain
COXE_MOUSE	--	1	1	2	--	Cytochrome c oxidase polypeptide VIa-liver
FUMH_MOUSE	--	--	--	--	2	Fumarate hydratase, mitochondrial precursor
IDHG_MOUSE	--	1	--	--	--	Isocitrate dehydrogenase
MDHM_MOUSE	7	1	2	9	11	Malate dehydrogenase
NNTM_MOUSE	--	--	--	--	2	NAD(P) transhydrogenase
SODM_MOUSE	1	4	5	9	4	Superoxide dismutase
UCR2_MOUSE	--	--	--	1	1	Ubiquinol-cytochrome C reductase complex core protein 2
calcium ion binding [GO:0005509]						
ATA2_MOUSE	--	--	1	--	--	Sarcoplasmic/endoplasmic reticulum calcium ATPase 2
ATA3_MOUSE	--	--	--	1	3	Sarcoplasmic/endoplasmic reticulum calcium ATPase 3
CALX_MOUSE	2	5	10	9	6	Calnexin precursor
CAQ1_MOUSE	--	--	--	--	3	Calsequestrin, skeletal muscle isoform precursor
CAQ2_MOUSE	--	--	--	1	--	Calsequestrin, cardiac muscle isoform precursor
FBL1_MOUSE	--	3	--	--	--	Fibulin-1 precursor
FBL2_MOUSE	2	2	4	3	16	Fibulin-2 precursor
KPCA_MOUSE	--	2	3	2	--	Protein kinase C, alpha type
NID2_MOUSE	1	4	1	2	17	Nidogen-2 precursor
NIDO_MOUSE	--	2	--	--	2	Nidogen precursor
cell adhesion [GO:0007155]						
CADD_MOUSE	--	--	--	--	3	Cadherin-13 precursor
FINC_MOUSE	23	66	11	7	246	Fibronectin
ITA7_MOUSE	--	--	--	--	3	Integrin alpha-7 precursor
ITA5_MOUSE	3	4	2	6	5	Integrin alpha-5
ITAV_MOUSE	--	--	--	--	1	Integrin alpha-V precursor
cytoskeleton [GO:0005856]						
DAG1_MOUSE	--	1	--	--	4	Dystroglycan precursor
FAK1_MOUSE	--	--	--	1	--	Focal adhesion kinase 1
PLAK_MOUSE	--	1	--	--	--	Junction plakoglobin
SGCA_MOUSE	--	--	--	--	1	Alpha-sarcoglycan precursor
SGCB_MOUSE	--	1	--	1	3	Beta-sarcoglycan
SNA1_MOUSE	--	--	--	--	1	Alpha-1-syntrophin
VIME_MOUSE	27	38	32	54	126	Vimentin
muscle development [GO:0007517]						
ACTS_HUMAN	--	--	2	2	1	Actin, alpha skeletal muscle
DESM_MOUSE	3	1	7	11	38	Desmin
MLE1_MOUSE	--	1	2	3	6	Myosin light chain 1, skeletal muscle isoform
MYH6_MOUSE	--	5	4	4	5	Myosin heavy chain, cardiac muscle alpha isoform
MYHB_MOUSE	4	3	4	1	6	Myosin heavy chain, smooth muscle isoform
MYPH_MOUSE	--	--	4	2	--	Myosin-binding protein H
TPCC_MOUSE	--	--	--	--	2	Troponin C, slow skeletal and cardiac muscles
TRT2_MOUSE	--	--	1	1	2	Troponin T, cardiac muscle isoforms
KCRM_MOUSE	--	--	--	2	1	Creatine kinase, M chain

Table 5:

Functional categories [GO-terms] Proteins identified	MB	2d	4d	6d	10d	Description
cell cycle [GO:0007049]						
CCT1_MOUSE	1	2	8	7		Cyclin T1
CKS1_HUMAN	2	--	--	--	--	Cyclin-dependent kinases regulatory subunit 1
CUL3_MOUSE	2	--	--	--	--	Cullin homolog 3
SEP2_MOUSE	27	29	15	12	8	Septin 2
SEP5_MOUSE	2	1	--	--	--	Septin 5
SEP6_MOUSE	7	--	1	--	--	Septin 6
SEP7_MOUSE	38	18	5	2	2	Septin 7
Q9QYX9	17	3	3	1	--	Septin-like protein Sint1
DNA replication [GO:0006260]						
CAFA_MOUSE	1	--	--	--	--	Chromatin assembly factor 1 subunit A
DPO2_MOUSE	1	--	--	--	--	DNA polymerase alpha 70 kDa subunit
MCM2_MOUSE	2	2	--	1	--	DNA replication licensing factor MCM2
MCM3_MOUSE	1	2	--	--	--	DNA replication licensing factor MCM3
MCM4_MOUSE	2	--	--	--	--	DNA replication licensing factor MCM4
MCM6_MOUSE	2	--	--	--	--	DNA replication licensing factor MCM6
MCM7_MOUSE	1	1	1	2	--	DNA replication licensing factor MCM7
RBB4_MOUSE	5	5	2	2	--	Chromatin assembly factor 1 subunit C
chromatin [GO:0000785]						
HDA1_MOUSE	5	1	1	1	--	Histone deacetylase 1
HMG1_MOUSE	48	41	12	14	2	High mobility group protein 1
HMG2_MOUSE	19	8	5	1	--	High mobility group protein 2
MRC1_MOUSE	14	5	--	--	--	SWI/SNF related matrix-associated actin-dependent regulator of chromatin subfamily C member 1
O55047	2	1	--	--	--	TOUSLED-like kinase
transcriptional repressor activity [GO:0016564]						
FXP1_MOUSE	3	1	1	--	--	Forkhead box protein P1
Q9R190	2	1	--	1	--	Metastasis associated protein MTA2
RBB7_MOUSE	2	11	--	--	--	Histone acetyltransferase type B subunit 2
SIP1_MOUSE	1	2	2	1	--	Zinc finger homeobox protein 1b
DNA topoisomerase activity [GO:0003916]						
TP2A_MOUSE	1	1	--	--	--	DNA topoisomerase II, alpha isozyme
TP2B_MOUSE	1	3	2	2	--	DNA topoisomerase II, beta isozyme

Table 6:

Functional categories [GO-terms] Proteins identified	MB	2d	4d	6d	10d	Description
mitochondrion [GO:0005739]						
ETFA_MOUSE	--	--	--	--	1	Electron transfer flavoprotein alpha-subunit
ETFB_MOUSE	--	--	--	--	1	Electron transfer flavoprotein beta-subunit
HCDH_MOUSE	--	--	--	--	8	Short chain 3-hydroxyacyl-CoA dehydrogenase
PDX5_MOUSE	--	--	--	--	7	Peroxiredoxin 5
UCRH_MOUSE	--	--	--	--	1	Ubiquinol-cytochrome C reductase complex 11 kDa protein
oxidoreductase activity [GO:0016491]						
DHA4_MOUSE	--	--	--	--	1	Fatty aldehyde dehydrogenase
HO1_MOUSE	--	--	--	--	3	Heme oxygenase 1
PDX3_MOUSE	--	--	--	--	3	Thioredoxin-dependent peroxide reductase
PGH1_MOUSE	--	--	--	--	1	Prostaglandin G/H synthase 1 precursor
electron transport [GO:0006118]						
ACDL_MOUSE	--	--	--	--	3	Acyl-CoA dehydrogenase, long-chain specific
ACDS_MOUSE	--	--	--	--	2	Acyl-CoA dehydrogenase, short-chain specific
ACDV_MOUSE	--	--	--	--	1	Acyl-CoA dehydrogenase, very-long-chain specific
CY1_MOUSE	--	--	--	--	3	Cytochrome c1, heme protein, mitochondrial precursor
NNTM_MOUSE	--	--	--	--	2	NAD(P) transhydrogenase, mitochondrial precursor
NOS2_MOUSE	--	--	--	--	2	Nitric oxide synthase, inducible
cell adhesion [GO:0007155]						
CADD_MOUSE	--	--	--	--	3	Cadherin-13 precursor
ITAV_MOUSE	--	--	--	--	1	Integrin alpha-V precursor
LMB1_MOUSE	--	--	--	--	1	Laminin beta-1 chain precursor
CD9_MOUSE	--	--	--	--	2	CD9 antigen
VTNC_MOUSE	--	--	--	--	2	Vitronectin precursor
fatty acid metabolism [GO:0006631]						
CAO1_MOUSE	--	--	--	--	1	Acyl-coenzyme A oxidase 1
HCDH_MOUSE	--	--	--	--	8	Short chain 3-hydroxyacyl-CoA dehydrogenase
LCFC_MOUSE	--	--	--	--	1	Long-chain-fatty-acid--CoA ligase 3
Q8QZU4	--	--	--	--	2	Similar to hydroxyacyl-coenzyme A dehydrogenase